



Short communication

Influences of carbon support on the electrocatalysis of polypyrrole-modified cobalt hydroxide in the direct borohydride fuel cell

Haiying Qin, Zixuan Liu, Shaojiang Lao, Jingke Zhu, Zhoupeng Li*

Department of Chemical and Biological Engineering, Zhejiang University, Zeda Road 38, Hangzhou 310027, Zhejiang, PR China

ARTICLE INFO

Article history:

Received 22 September 2009

Received in revised form 1 December 2009

Accepted 1 December 2009

Available online 4 December 2009

Keywords:

Carbon support

Electrocatalytic activity

Direct borohydride fuel cell

Cobalt hydroxide

Performance

ABSTRACT

Catalysts of $\text{Co}(\text{OH})_2$ supported on polypyrrole-modified Super P carbon and on polypyrrole-modified BP 2000 carbon are prepared by a chemical method. The structure and morphology of the catalysts are characterized by X-ray diffraction, X-ray photoemission spectroscopy and transmission electron microscopy. BP 2000 carbon demonstrates larger specific surface area, lower crystallization degree and lower electrochemical resistance than Super P carbon. The surface characteristics of the carbon support have notable influences on the morphology and electrocatalytic activity of $\text{Co}(\text{OH})_2$. $\text{Co}(\text{OH})_2$ distributes much homogeneously on the polypyrrole-modified BP 2000 with more polypyrrole content, and exhibits higher electrocatalytic activity compared with that on polypyrrole-modified Super P carbon. The DBFC using $\text{Co}(\text{OH})_2$ supported on polypyrrole-modified BP 2000 as the catalysts demonstrates fairly good performance (160 mW cm^{-2}) under ambient conditions.

© 2009 Elsevier B.V. All rights reserved.

1. Introduction

The direct borohydride fuel cell (DBFC) has attracted much interest as a potential power source for portable and mobile applications due to its higher electromotive force of 1.64 V and higher capacity of 5.67 Ah g^{-1} than proton exchange membrane fuel cell and direct methanol fuel cell [1,2]. Unlike those fuel cells working under an acidic electrolyte, DBFCs operate under alkaline electrolytes so that non-precious metals can be used as catalysts for borohydride oxidation reaction (BOR) and oxygen reduction reaction (ORR) because BOR and ORR are more favorable in alkaline condition [3,4]. However, DBFCs using alkaline NaBH_4 solutions as the fuel have to keep a chemical balance of NaOH due to that Na^+ functions as a charge carrier to form NaOH solution at cathode side during operation [5]. It is considered that this problem can be resolved by recycling NaOH solutions with a pump from cathode side to anode side. In recycling NaOH solutions, how to avoid the conductivity degradation of NaOH solutions caused by CO_2 absorption would be another problem in development of the DBFC technology.

Carbon supported metal macrocycle compounds such as carbon supported Co polypyrrole [6], carbon supported Co and Fe phthalocyanines [7,8] are considered to be alternatives to Pt/C as cathode catalysts due to their good electrocatalytic activities comparable to Pt/C. It has been proved that the characteristics of carbon support

significantly influence the electrocatalytic activity and stability of metal macrocycle compounds [9–12]. For example, the dispersion and the surface composition of metal macrocycle compounds are dependent upon the surface properties of carbon support. The conductivity of carbon support plays an important role in improving electrocatalysis [13].

Super P is a kind of conventional carbon black which is usually used as conducting additive in lithium-ion batteries [14]. In our previous work [15], we studied the electrocatalytic properties of $\text{Co}(\text{OH})_2$ supported on polypyrrole-modified Super P carbon. It is considered that the specific surface area of Super P is notably lower than that of other carbon supports such as Vulcan XC-72 or BP 2000 [16].

By using Super P and BP 2000 as a pair of comparison objectives, this work investigates the influences of carbon support on the electrocatalytic activities of $\text{Co}(\text{OH})_2$ supported on polypyrrole-modified carbon.

2. Materials and methods

2.1. Catalyst preparation

The carbon dispersion was prepared by adding 10 g of carbon powder (Super P or BP 2000) and 2.5 mL of glacial acetic acid to 150 mL of de-ionized water and then stirring for 20 min under room temperature. After that, 2 g of pyrrole and 10 mL of H_2O_2 solution (10 wt.%) were added to the carbon dispersion. The mixture was stirred under room temperature for 3 h to form polypyrrole on carbon particles. The pH value of the solution was controlled to be

* Corresponding author. Tel.: +86 571 87951977; fax: +86 571 87953149.
E-mail address: zhoupengli@zju.edu.cn (Z. Li).

around 3. The polypyrrole-loaded carbon powders were filtered, washed and then dried at 90 °C under vacuum for 10 h. The loading of polypyrrole on the carbon was about 17 wt.%.

3 g of the polypyrrole-loaded carbon powders was placed in a three-necked round-bottom flask and intimately mixed with 15 mL of $\text{Co}(\text{NO}_3)_2$ solution (10 wt.%). Then the mixture was stirred for 30 min at 80 °C. After that, 400 mL of NaOH solution (1 wt.%) was added into the mixture at a rate of 20 mL min⁻¹ with a peristaltic pump. The catalysts were obtained after filtering and washing repeatedly with warm de-ionized water, and then drying at 90 °C under vacuum for 12 h. The loading of $\text{Co}(\text{OH})_2$ was calculated to be about 15 wt.%.

2.2. Electrode preparation

Cathodes were prepared by coating catalyst slurry on to a piece of hydrophobic carbon cloth with a catalyst loading of 5 mg cm⁻². Anodes were prepared by coating the catalyst slurry on to a piece of Ni foam with a catalyst loading of 5 mg cm⁻². The catalyst slurry was prepared by mixing the catalyst with de-ionized water, Nafion solution (5 wt.%) and anhydrous ethanol with a mass ratio of 1:3:7:3.

2.3. Characterization and measurement

The specific surface area of catalysts and carbon supports was determined by Brunauer–Emmett–Teller (BET) isotherm method with N₂ adsorption under the liquid-nitrogen temperature using Coulter OMNISORP-100CX instrument. The samples were degassed to 10⁻⁵ Pa for 2 h at 200 °C before testing. The crystal structure of catalysts was identified by X-ray diffraction (XRD) with Rigaku-D/MAX-2550PC diffractometer using Cu K α radiation ($\lambda = 1.5406 \text{ \AA}$). The chemical valence states of Co and N were identified by X-ray photoemission spectroscopy (XPS) (PHI-5000C ESCA system). The morphologies of catalysts and carbon particles were observed with a JEM-2010 transmission electron microscopy (TEM) operated at 200 kV.

A single cell with an active area of 6 cm² was assembled to evaluate the electrocatalytic activity of the catalysts in the DBFC. The cell configuration was described in our previous paper [15]. The Nafion membrane N112 was used as the electrolyte. An alkaline NaBH₄ solution (5 wt.% of NaBH₄, 10 wt.% of NaOH) was used as the fuel. An Hg/HgO (1 M NaOH) electrode was applied as the reference electrode which was connected with the fuel tank by a salt bridge. The cell performance and electrode polarization were measured at a fuel flow rate of 10 mL min⁻¹ and a dry O₂ flow rate of 150 mL min⁻¹ under ambient conditions.

Electrochemical impedance spectroscopy (EIS) analyses and rotating disc electrode (RDE) voltammetry tests were carried out on a Zahner IM6 analyzer using Hg/HgO electrode as the reference electrode in a three-electrode system. The AC frequency was varied from 10 mHz to 10 kHz with an amplitude of 5 mV. The experimental setup and procedure of RDE voltammetry were described in detail elsewhere [17]. A Pt wire electrode was used as the counter electrode. The working electrode was prepared as following: 8.0 mg of catalyst sample, 1.5 mL of ethanol and 0.1 mL of Nafion solution (5 wt.%) were ultrasonically mixed to form homogenous ink. Then 20 μL of this ink was pipetted on to the pretreated glassy carbon electrode (3 mm in diameter) and dried at room temperature. RDE voltammograms were recorded between -1.0 and 0.2 V (vs. Hg/HgO) in 0.1 M KOH solution saturated with O₂ under room temperature at a scan rate of 10 mV s⁻¹ and a rotation speed of 200, 400, 600 and 800 rpm, respectively.

3. Results and discussion

3.1. Catalyst characterization

As shown in Fig. 1, TEM images reveal the difference in morphology between Super P carbon and BP 2000 carbon. Super P particle has smooth surface with an average size of around 40 nm, while BP 2000 particle shows rough surface with an average size of around 20 nm. The high resolution transmission electron microscopy (HRTEM) observations indicate that the crystallization degree of BP 2000 is lower than that of Super P. From BET measurement, the specific surface area of Super P is determined to be 58 m² g⁻¹, which is much lower than that of BP 2000 (1443 m² g⁻¹). This result is consistent to the TEM observation.

Fig. 2 shows the XRD patterns of the as-prepared $\text{Co}(\text{OH})_2$ supported on polypyrrole-modified Super P carbon ($\text{Co}(\text{OH})_2$ -PPY-SP) and on polypyrrole-modified BP 2000 carbon ($\text{Co}(\text{OH})_2$ -PPY-BP). The XRD diffraction peaks at 19.1°, 32.4°, 37.9° and 51.3° correspond to the (0 0 1), (1 0 0), (1 0 1) and (1 0 2) crystalline planes of β - $\text{Co}(\text{OH})_2$, respectively. Widening of XRD diffraction peak of carbon at 26.1° reveals that BP 2000 carbon has low crystallization degree, and the shifting of the peak to smaller angle implies that BP 2000 carbon has larger interplanar spacing than Super P carbon. The result is consistent to the HRTEM observations as shown in Fig. 1.

Morphologies of the prepared $\text{Co}(\text{OH})_2$ -PPY-SP and $\text{Co}(\text{OH})_2$ -PPY-BP are shown in Fig. 3. It can be seen that there are some platelets dispersed on carbon particles. The platelets are smaller in size and distributed more homogeneously on BP 2000 carbon than those on Super P carbon. Park and Keane [18] have found that the strong epitaxial interaction between the catalytic species and the graphitic planes leads to a homogeneous distribution of the loaded Pd. It is considered that the rough surface, large interplanar spacing and high specific surface area of BP 2000 would enhance the epitaxial interaction between $\text{Co}(\text{OH})_2$ and the graphitic planes. As a result, $\text{Co}(\text{OH})_2$ can be distributed homogeneously on the BP 2000 carbon with smaller size than that on the Super P carbon.

Co and N electron binding energies on the surfaces of $\text{Co}(\text{OH})_2$ -PPY-SP and $\text{Co}(\text{OH})_2$ -PPY-BP are investigated by XPS analysis as shown in Fig. 4. Electron binding energy values of Co 2p_{1/2} and Co 2p_{3/2} reveal that the chemical valence of Co is +2 in these catalysts, which is consistent with the XRD result and former studies [19]. It is noted that the peak of Co 2p_{3/2} shifts from 781.0 to 785 eV in both $\text{Co}(\text{OH})_2$ -PPY-SP and $\text{Co}(\text{OH})_2$ -PPY-BP. The similar phenomenon was also observed in the study of Co-PPY/C [20]. Zhang and Bai [21] reported that N 1s electron binding energy in polypyrrole was 399 eV. From Fig. 4(b), it can be seen that the N 1s electron binding energy in $\text{Co}(\text{OH})_2$ -PPY-SP and $\text{Co}(\text{OH})_2$ -PPY-BP are higher than 399 eV. The energy shifts of Co 2p_{3/2} and N 1s electrons imply that Co is binding to N in the $\text{Co}(\text{OH})_2$ -PPY-SP and $\text{Co}(\text{OH})_2$ -PPY-BP.

In addition, the N 1s peak intensity of $\text{Co}(\text{OH})_2$ -PPY-BP is larger than that of $\text{Co}(\text{OH})_2$ -PPY-SP. As N is only from polypyrrole, it is implied that BP 2000 carbon can absorb more polypyrrole than Super P carbon because BP 2000 carbon has larger specific surface area and lower crystallization degree. Through BET measurements, it was found that polypyrrole-modified Super P carbon exhibited a specific surface area (60 m² g⁻¹) which was equivalent to that of the original Super P carbon (58 m² g⁻¹). However, the specific surface area of polypyrrole-modified BP 2000 carbon (664 m² g⁻¹) was reduced nearly 50% compared with that of the original BP 2000 carbon (1443 m² g⁻¹). BET results indirectly reconfirmed that BP 2000 carbon absorbed more polypyrrole than Super P carbon. Consequently, $\text{Co}(\text{OH})_2$ -PPY-BP contained more polypyrrole than $\text{Co}(\text{OH})_2$ -PPY-SP.

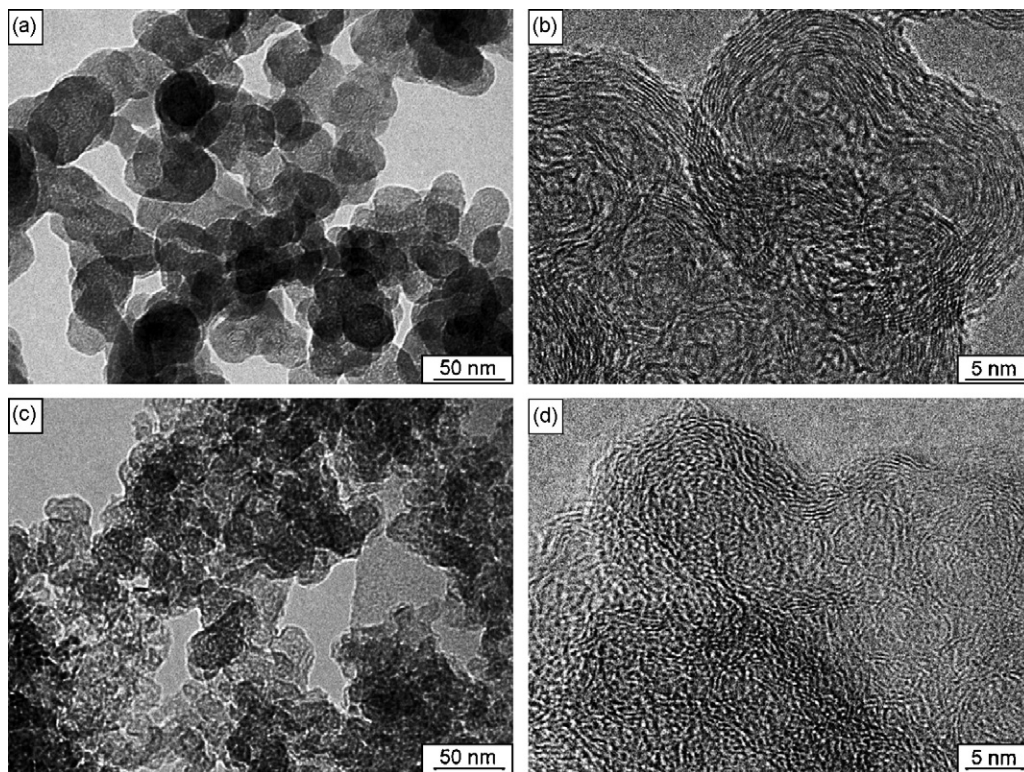


Fig. 1. TEM and HRTEM images of Super P carbon (a and b) and BP 2000 carbon (c and d).

3.2. Cell performance

Performances of the test cells using Co(OH)_2 -PPY-SP or Co(OH)_2 -PPY-BP as the catalysts are illustrated in Fig. 5. Compared with the cell using Co(OH)_2 -PPY-SP, the cell using Co(OH)_2 -PPY-BP demonstrates better performance. Although the cell using Co(OH)_2 -PPY-SP has approximate open-circuit voltage with the cell using Co(OH)_2 -PPY-BP, the polarization of the cell using Co(OH)_2 -PPY-SP is worse than that of the cell using Co(OH)_2 -PPY-BP. As a result, the maximum power density of the cell using Co(OH)_2 -PPY-BP (160 mW cm^{-2}) is 28% higher than that of the cell

using Co(OH)_2 -PPY-SP (126 mW cm^{-2}). Furthermore, the electrode polarization measurements indicate that the slopes of the linear potential-current relations corresponding to Co(OH)_2 -PPY-BP cathode and anode are smaller than those of the linear potential-current relations corresponding to the Co(OH)_2 -PPY-SP cathode and anode, as shown in Fig. 6.

Fig. 7 shows the electrochemical impedance spectra of the anode and the cathode at open circuit condition in a three-electrode system. It can be seen that the modulus of anode impedance is about 10 times smaller than that of the cathode impedance, showing that the performance of the DBFC is mainly determined by the ORR process. The impedance spectra of cathodes demonstrate a single impedance arc in the Nyquist plot as shown in Fig. 7(a). The diameter of the single semicircle loop is a measure of the charge transfer resistance of the ORR [22]. There are two arcs in the Nyquist plot of anodes as shown in Fig. 7(b). The diameter of semicircle at low frequencies is attributed to the charge transfer resistance of BOR [23]. It can be seen that both cathode and anode using Super P carbon as the catalysts support exhibit larger charge transfer resistance than those using BP 2000 carbon. Considering the results obtained from polarization measurements as shown in Fig. 6, it can be concluded that the use of BP 2000 carbon as the catalyst support can decrease the electrode polarization of the PPY modified Co(OH)_2 catalysts due to the decrease of charge transfer resistance, so that the cell performance can be improved.

As a comparison, we measured the electrochemical impedance spectra of anode and cathode using Super P carbon and BP 2000 carbon without PPY modification and Co(OH)_2 loading. The results demonstrated that BP 2000 carbon had lower electrochemical reaction resistance as shown in Fig. 7(c) and (d).

Zhang et al. [24] suggested using apparent exchange current density ($i_{\text{O}_2}^0$) to evaluate the electrocatalysis through establishment of an equivalent circuit and simulation of the Nyquist plots. Accord-

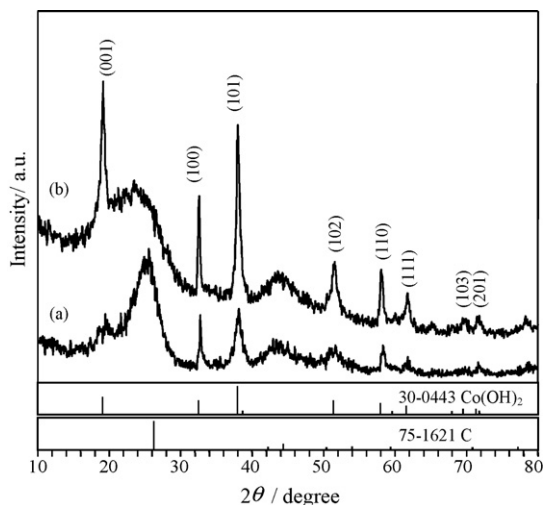


Fig. 2. XRD patterns of the as-prepared Co(OH)_2 -PPY-SP (a) and Co(OH)_2 -PPY-BP (b).

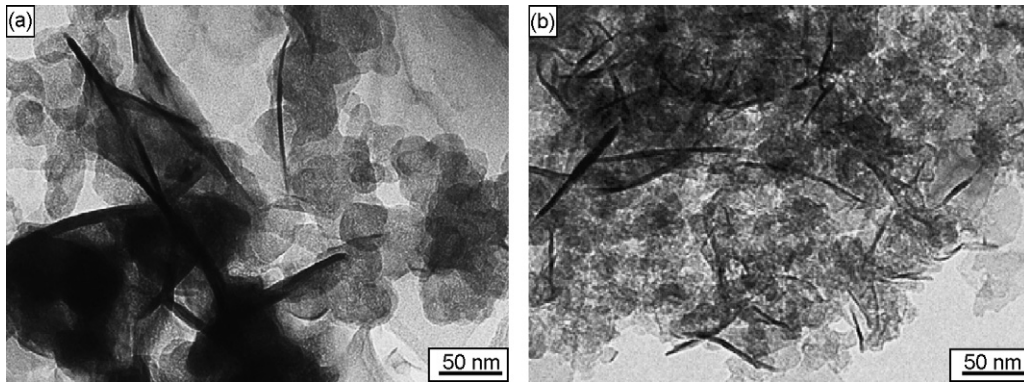


Fig. 3. TEM images of Co(OH)₂-PPY-SP (a) and Co(OH)₂-PPY-BP (b).

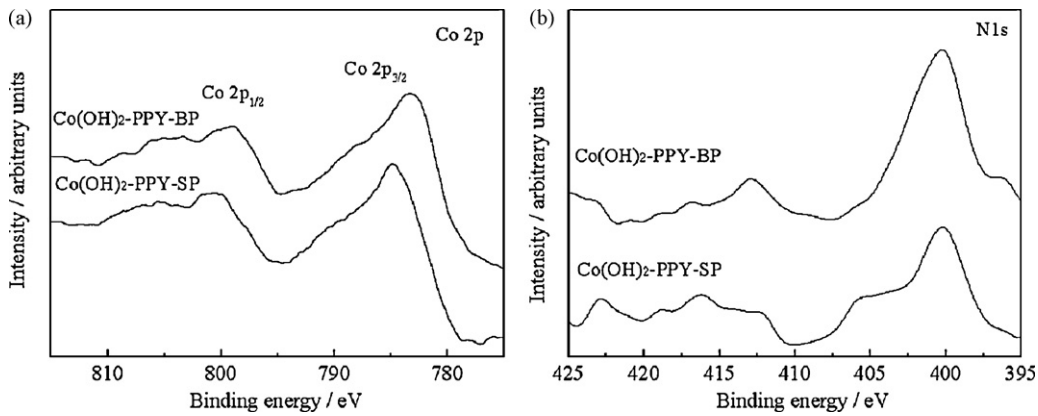


Fig. 4. Co 2p (a) and N 1s (b) core-level XPS spectra of Co(OH)₂-PPY-SP and Co(OH)₂-PPY-BP.

ing to Eq. (1), the apparent exchange current densities for ORR can be evaluated.

$$R^{OCV} = \frac{RT}{n_{\alpha O} F i_{O_2}^0} \quad (1)$$

where R is the universal gas constant ($8.314 \text{ J mol}^{-1} \text{ K}^{-1}$), T is the temperature (K), $n_{\alpha O}$ is the electron transfer numbers related to ORR.

The $n_{\alpha O}$ values corresponding to Co(OH)₂-PPY-SP and Co(OH)₂-PPY-BP cathode were determined to be 2.9 and 3.7, respectively,

which are calculated by Koutecky–Levich plots according to the RDE voltammograms as shown in Fig. 8. The corresponding R^{OCV} values were obtained from the diameter of the semicircle at the low frequency in Fig. 7(a). According to Eq. (1), the apparent exchange current densities of ORR at Co(OH)₂-PPY-SP and Co(OH)₂-PPY-BP cathode are calculated to be $2.77 \times 10^{-4} \text{ A cm}^{-2}$ and $3.54 \times 10^{-4} \text{ A cm}^{-2}$, respectively, which reveals that ORR demonstrates faster kinetics on Co(OH)₂-PPY-BP. It is considered that the homogeneous dispersion of Co(OH)₂ on polypyrrole-modified BP 2000, provides more active sites for the electrochemical reactions so that ORR kinetics is improved.

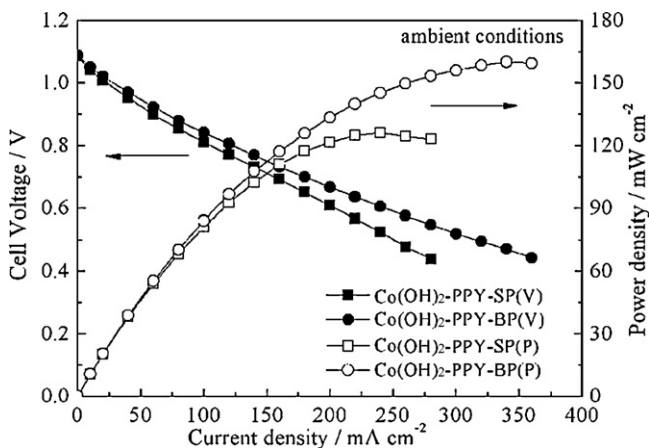


Fig. 5. Cell performance of DBFCs using Co(OH)₂-PPY-SP or Co(OH)₂-PPY-BP as the catalysts under ambient conditions.

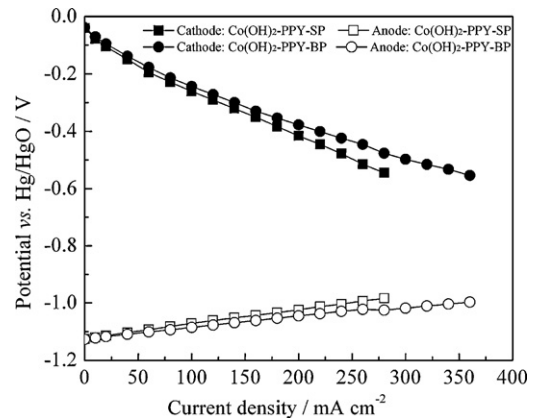


Fig. 6. Cathode and anode polarization curves of DBFCs using Co(OH)₂-PPY-SP or Co(OH)₂-PPY-BP as the catalysts under ambient conditions.

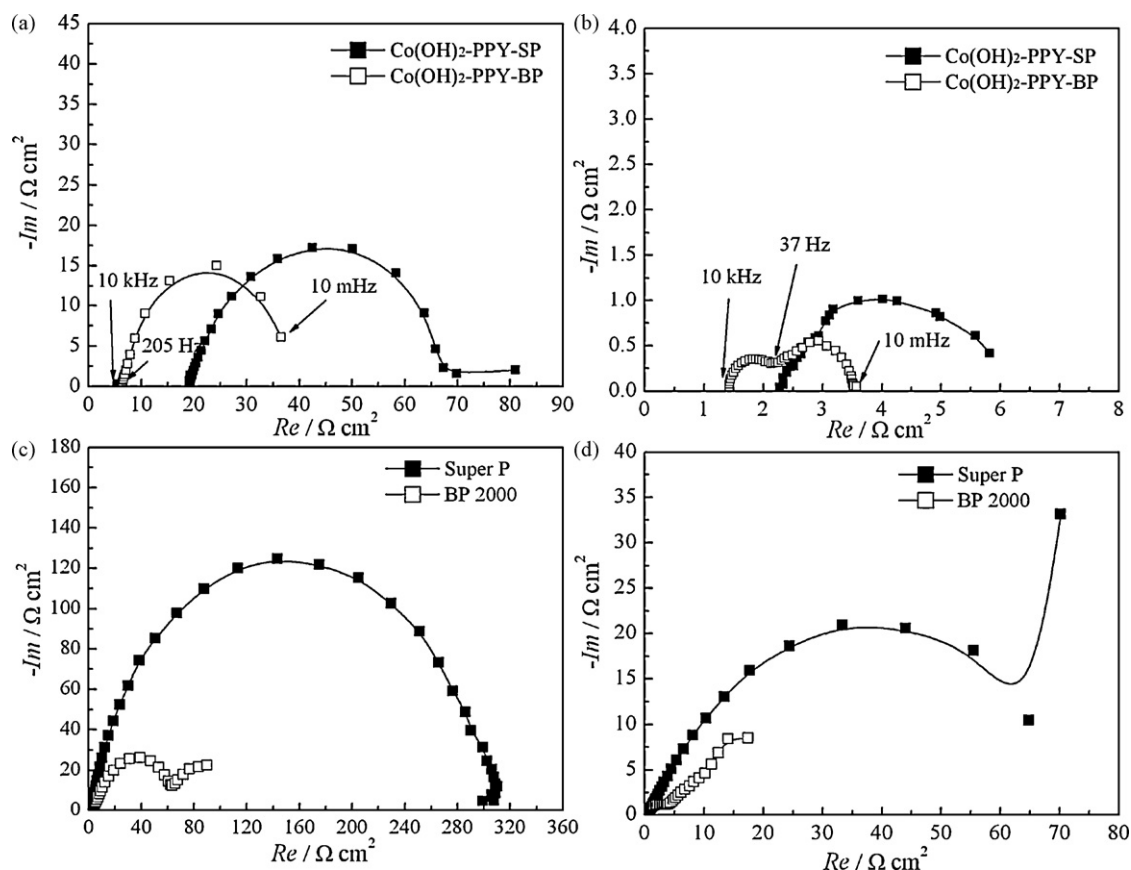


Fig. 7. Electrochemical impedance spectra for the cathodes of $\text{Co(OH)}_2\text{-PPY-SP}$ and $\text{Co(OH)}_2\text{-PPY-BP}$ (a); the anodes of $\text{Co(OH)}_2\text{-PPY-SP}$ and $\text{Co(OH)}_2\text{-PPY-BP}$ (b), the cathodes of Super P carbon and BP 2000 carbon (c); the anodes of Super P carbon and BP 2000 carbon (d).

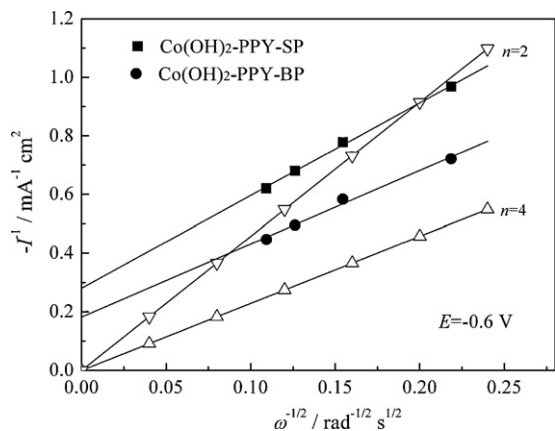


Fig. 8. Koutecky–Levich plots at -0.6 V obtained at $\text{Co(OH)}_2\text{-PPY-SP/GC}$ and $\text{Co(OH)}_2\text{-PPY-BP/GC}$ electrode in O_2 saturated 0.1 M KOH solutions at room temperature. The theoretical slopes calculated assuming the 2- and 4-electron processes for the O_2 reduction are given.

4. Conclusions

Based on the microstructure and morphology studies to $\text{Co(OH)}_2\text{-PPY-SP}$ and $\text{Co(OH)}_2\text{-PPY-BP}$, and investigations of their electrochemical catalytic activities, several conclusions can be drawn as follows:

(1) The characteristics of carbon support demonstrate notable influences on the morphology and the electrocatalytic activity of the polypyrrole-modified carbon supported Co(OH)_2 .

- (2) BP 2000 carbon demonstrates larger specific surface area and lower electrochemical resistance than Super P carbon. Co(OH)_2 could distribute much homogeneously on the polypyrrole-modified BP 2000 carbon. The prepared $\text{Co(OH)}_2\text{-PPY-BP}$ contains more polypyrrole than $\text{Co(OH)}_2\text{-PPY-SP}$.
- (3) $\text{Co(OH)}_2\text{-PPY-BP}$ demonstrates lower charge transfer resistance towards BOR and faster ORR kinetics than $\text{Co(OH)}_2\text{-PPY-SP}$. The use of BP 2000 as carbon support could effectively decrease the electrochemical resistance of the electrodes in DBFCs so that the DBFC using $\text{Co(OH)}_2\text{-PPY-BP}$ as catalyst demonstrates higher power density than the cell using $\text{Co(OH)}_2\text{-PPY-SP}$.

Acknowledgements

This work is financially supported by Hi-tech Research and Development Program of China (863), grant no. 2007AA05Z144, Doctoral fund from Education ministry of China (20070335003), and the National Natural Science Foundation of China (20976156).

References

- [1] Z.P. Li, B.H. Liu, K. Arai, S. Suda, J. Alloys Compd. 404 (2005) 648–652.
- [2] U.B. Demirci, J. Power Sources 169 (2) (2007) 239–246.
- [3] B.H. Liu, Z.P. Li, J. Power Sources 187 (2009) 291–297.
- [4] U.B. Demirci, J. Power Sources 172 (2) (2007) 676–687.
- [5] Z.P. Li, B.H. Liu, K. Arai, S. Suda, J. Electrochem. Soc. 150 (2003) A868–872.
- [6] H.Y. Qin, Z.X. Liu, W.X. Yin, J.K. Zhu, Z.P. Li, J. Power Sources 185 (2) (2008) 909–912.
- [7] J.F. Ma, Y.N. Liu, P. Zhang, J. Wang, Electrochem. Commun. 10 (1) (2008) 100–102.
- [8] J.F. Ma, J. Wang, Y.N. Liu, J. Power Sources 172 (2007) 220–224.
- [9] A. Widelov, R. Larsson, Electrochim. Acta 37 (2) (1992) 187–197.
- [10] G. Wei, J.S. Wainright, R.F. Savinell, J. New Mater. Electrochem. Syst. 3 (2) (2000) 121–129.

- [11] F. Jaouen, S. Marcotte, J.P. Dodelet, G. Lindbergh, J. Phys. Chem. B 107 (6) (2003) 1376–1386.
- [12] C. Medard, M. Lefevre, J.P. Dodelet, F. Jaouen, G. Lindbergh, Electrochim. Acta 51 (16) (2006) 3202–3213.
- [13] W.Q. Yang, S.H. Yang, J.S. Guo, G.Q. Sun, Q. Xin, Carbon 45 (2) (2007) 397–401.
- [14] K.T. Nam, D.W. Kim, P.J. Yoo, C.Y. Chiang, N. Meethong, P.T. Hammond, Y.M. Chiang, A.M. Belcher, Science 312 (5775) (2006) 885–888.
- [15] H.Y. Qin, Z.X. Liu, L.Q. Ye, J.K. Zhu, Z.P. Li, J. Power Sources 192 (2) (2009) 385–390.
- [16] F. Jaouen, F. Charreteur, J.P. Dodelet, J. Electrochem. Soc. 153 (2006) A689–A698.
- [17] D. Zhang, D. Chi, T. Okajima, T. Ohsaka, Electrochim. Acta 52 (17) (2007) 5400–5406.
- [18] C. Park, M.A. Keane, J. Colloid Interf. Sci. 266 (1) (2003) 183–194.
- [19] A.A. Khassin, T.M. Yurieva, V.V. Kaichev, V.I. Bukhtiyarov, A.A. Budneva, E.A. Paukshtis, V.N. Parmon, J. Mol. Catal. A: Chem. 175 (1/2) (2001) 189–204.
- [20] M. Yuasa, A. Yamaguchi, H. Itsuki, K. Tanaka, M. Yamamoto, K. Oyaizu, Chem. Mater. 17 (17) (2005) 4278–4281.
- [21] X. Zhang, R. Bai, Langmuir 18 (9) (2002) 3459–3465.
- [22] X.Z. Yuan, H.J. Wang, J.C. Sun, J.J. Zhang, Int. J. Hydrogen Energy 32 (17) (2007) 4365–4380.
- [23] B.H. Liu, Z.P. Li, K. Arai, S. Suda, Electrochim. Acta 50 (18) (2005) 3719–3725.
- [24] J.L. Zhang, Y.H. Tang, C.J. Song, J.J. Zhang, H.J. Wang, J. Power Sources 163 (1) (2006) 532–537.